

that the Co clusters are sufficiently small that they are not truly bulk in nature. It is likely that these particles are single domain. The smaller Co particles were characterized by a spectrum with broader peaks than those of the large clusters and with a central peak located at 212 MHz. A secondary peak located at 222 MHz is clearly evident. Again, these two peaks might indicate fcc- and hcp-like short-range order, with the downward shift in frequency

and the additional broadening being consequences of the fact that these clusters are also single domain and even further removed from the bulk situation.

The work presented here clearly demonstrates how NMR techniques can provide valuable information concerning the size and location of magnetically-ordered metallic clusters encaged in zeolite materials.

Influence of Strain on Chemical Reactivity. Relative Reactivity of Torsionally Strained Double Bonds in 1,3-Dipolar Cycloadditions

Kenneth J. Shea* and Jang-Seob Kim

Contribution from the Department of Chemistry, University of California, Irvine, Irvine, California 92717. Received November 22, 1991

Abstract: The addition of picryl azide to a series of mono- and bicyclic olefins including *trans*-cycloalkenes and bridgehead alkenes is reported. Secondary reaction products were identified, and their mechanism of formation was explained by an analysis relating the transition state energies to the conformation of the reaction intermediates. Bridgehead alkenes showed reversed regiochemistry of cycloaddition when compared with model alkenes. It is proposed that the reversal of regiochemistry is caused by the out of plane bending of the bridgehead double bond. The kinetics of the cycloaddition reveals significant increases in reaction rate for the picryl azide addition to strained olefins. A good correlation was found in the plot of $\log k_{\text{rel}}$ vs ΔSE , where ΔSE values were calculated from differences of MM-2 steric energy between olefins and a model of the corresponding triazoline cycloadduct. This finding indicates that the strain relief in the transition state is a major factor affecting the reactivity of alkyl-substituted mono- and bicyclic olefins. The HOMO energy change did not affect the reactivity significantly in the picryl azide addition to alkyl-substituted olefins as evidenced by the absence of correlation in $\log k_{\text{rel}}$ vs ionization potential. Up to 60% of the steric energy difference (ΔSE) is found to be relieved in the transition state from the slope of the $\log k_{\text{rel}}$ vs ΔSE plots. By comparison of the reaction rates for the MCPBA epoxidation and the picryl azide addition, reactivity patterns were found to be similar among the olefins studied except for norbornene. An attempt was made to explain the norbornene anomaly by calling attention to the torsional interactions that develop between forming bonds and existing carbon-carbon bonds in the methylene bridge. An important outcome of this research is the quantification of the effect of strain on chemical reactivity and selectivity. The olefin strain changes both the rate of reaction and regiochemistry of the cycloaddition.

Introduction

In an effort to establish quantitative relationships between strain and reactivity,¹ we have undertaken a series of investigations of the rates of addition to torsionally distorted carbon-carbon double bonds. The present study examines the rates of azide addition to various strained alkenes. Organic azides react with olefins to form 1,2,3- Δ^2 -triazolines, a reaction first reported by Wolff in 1912.² The reaction is an important synthetic route to triazolines and their derivatives.³



R = Aryl, Aryl sulfonyl, CN etc.

In 1931, Alder and Stein observed that norbornene derivatives have high reactivity with phenyl azide.^{4,5} The ease of phenyl azide addition was subsequently employed as a measure of ring strain.

Several studies have since attempted to identify the origin of the high reactivity of the norbornene ring system.⁶

Azide additions to double bonds were recognized as an example of a 1,3-dipolar cycloaddition reaction from the extensive research of Huisgen.^{7,8} The general mechanistic features³ are a concerted but nonsynchronous cycloaddition. Reactivity may be viewed in FMO terms as an interaction of the highest occupied molecular orbital (HOMO) of the 1,3-dipole (or dipolarophile) with the lowest unoccupied molecular orbital (LUMO) of the dipolarophile (or 1,3-dipole).

The substituent effect on reactivity follows from the frontier orbital interaction between the azide and the olefin (Figure 1). Olefins having electron-donating or conjugating substituents have their major interaction between the LUMO of phenyl azide and the HOMO of the olefin, but olefins with electron-withdrawing substituents have their major interaction between the HOMO of phenyl azide and the LUMO of the olefin.⁹ The energy gap between the frontier orbital pairs becomes smaller as one progresses from parent ethylene to either electron-rich olefins or electron-deficient olefins, thus facilitating the reaction in both cases. When kinetic rate data are plotted against orbital energies ($\log k$ vs ionization potential), a characteristic U-shaped curve

(1) (a) Shea, K. J. *NATO ASI Ser., Ser. C* 1989, 273, 133-141. (b) Shea, K. J.; Kim, J.-S. *J. Am. Chem. Soc.* 1992, 114, 3044.

(2) Wolff, L. *Liebigs Ann. Chem.* 1912, 394, 23.

(3) Lwowski, W. In *1,3-Dipolar Cycloaddition Chemistry*; Padwa, A., Ed.; Wiley-Interscience: New York, 1984; Chapter 5.

(4) Alder, K.; Stein, G. *Liebigs Ann. Chem.* 1931, 485, 211.

(5) Alder, K.; Stein, G. *Liebigs Ann. Chem.* 1933, 501, 1.

(6) Huisgen, R. *Pure Appl. Chem.* 1980, 52, 2283.

(7) Huisgen, R. *Proc. Chem. Soc., London* 1961, 357.

(8) Huisgen, R. *Angew. Chem., Int. Ed. Engl.* 1963, 2, 565.

(9) Houk, K. N.; Sims, J.; Watts, C.; Luskus, L. *J. Am. Chem. Soc.* 1973, 95, 7301.

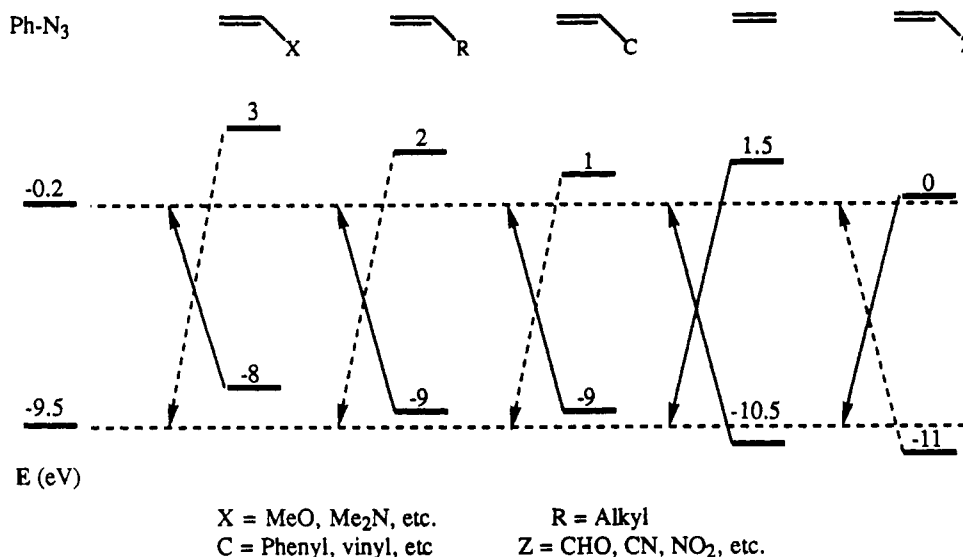


Figure 1. Frontier orbital energies for phenyl azide and substituted olefins.⁹

is observed in which both electron-rich and electron-deficient olefins have greater reactivities than the parent unsubstituted olefin, consistent with the prediction of frontier orbital theory.¹⁰

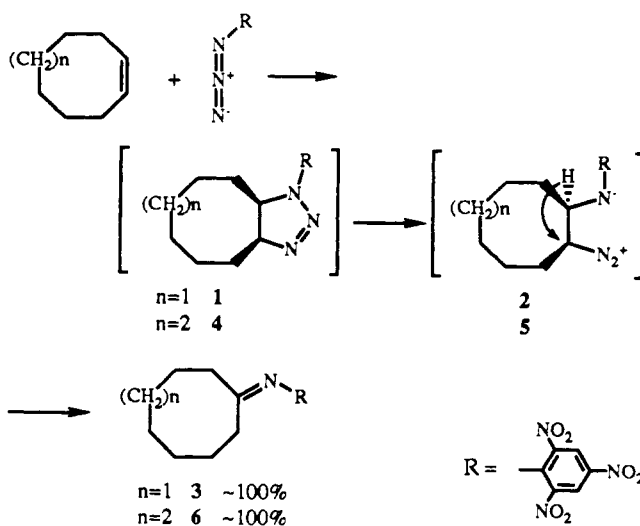
The regiochemistry of most azide additions also fits the prediction of FMO analysis.¹¹ Enamines,¹² enol ethers,¹³ and unsymmetrical alkenes¹⁴⁻¹⁶ give predominantly 5-substituted Δ^2 -triazolines. This is consistent with the dominant interaction between the azide LUMO and the olefin HOMO. Even cycloadditions with methylenecycloalkanes exhibit a preference toward the 1,5-regiochemistry,¹⁷ indicating that electronic factors often dominate steric effects. Styrene, however, produces a mixture of regioisomers with a slight excess of the 1,5-cycloadduct.¹⁸ Additions to methyl acrylate on the other hand produce a 4-substituted Δ^2 -triazoline cycloadduct as predicted by FMO analysis.¹⁹

In the present study, the absolute reaction rates of picryl azide addition in CHCl_3 with cyclic olefins, including strained *trans*-cycloalkenes and bridgehead olefins, were measured and their products were identified. The primary purpose of this work is to establish the relationship between chemical reactivity and strain. Picryl azide was selected because of its convenient rate of reaction with alkyl-substituted olefins. Molecular mechanics calculations (MM-2) were utilized to obtain quantitative measurements of strain energies of reactants and products. An additional goal of this work was to test the currently available FMO theory regarding the regiochemistry of cycloaddition to olefins containing torsionally distorted double bonds. The product compositions of azide additions to 1-methyl-*trans*-cyclooctene, bicyclo[3.3.1]non-1-ene, and bicyclo[4.3.1]dec-1(9)-ene were analyzed for this purpose.

Results

A. Product Analysis. All picryl azide (2,4,6-trinitrophenyl azide) additions were run at room temperature in CHCl_3 . Ratios reported in this section were determined by integration of ^1H -

Scheme I



NMR spectra of crude reaction mixtures. Isolated yields of preparative runs are given in the Experimental Section.

The picryl azide additions gave two secondary reaction products, imines and aziridines. In most cases, the primary cycloadduct triazolines were not detected. This is known to be the case in adducts with azides containing electron-withdrawing substituents.³ Characterization of product imines was accomplished by ^1H - and ^{13}C -NMR analysis, by comparison with the corresponding ketones, and by observation of the characteristic $\text{C}=\text{N}$ stretching band at approximately 1680 cm^{-1} in the IR spectra. Aziridines were also identified from their spectroscopic properties and by comparison of ^1H - and ^{13}C -NMR spectra with their corresponding epoxides prepared independently from the olefin. The imine products showed no syn-anti separation in either the ^1H - or ^{13}C -NMR spectra, consistent with time-averaged spectra.²⁰

cis-Cyclooctene and *cis*-cyclononene gave single products, cyclooctylidene-2,4,6-trinitroaniline (3) and cyclononylidene-2,4,6-trinitroaniline (6), respectively (Scheme I). These products arise from the decomposition of the triazolines followed by a 1,2-hydride shift in the corresponding zwitterions. Azide additions to simple *cis*-cycloalkenes gave similar products.^{21,22}

(10) Sustmann, R.; Trill, H. *Angew. Chem., Int. Ed. Engl.* **1972**, *11*, 838. Sustmann, R. *Pure Appl. Chem.* **1975**, *40*, 569.

(11) Fleming, I. *Frontier Orbitals and Organic Chemical Reactions*; Wiley: New York, 1976.

(12) Fusco, R.; Bianchetti, G.; Pocar, D.; Ugo, R. *Chem. Ber.* **1963**, *96*, 802.

(13) Huisgen, R.; Möbius, L.; Szeimies, G. *Chem. Ber.* **1965**, *98*, 1138.

(14) Scheiner, P. *Tetrahedron* **1967**, *24*, 349.

(15) Marsh, F.; Hermes, M. *J. Org. Chem.* **1972**, *37*, 2969.

(16) McManus, S.; Ortiz, M.; Abramovitch, R. *J. Org. Chem.* **1981**, *46*, 336.

(17) Wohl, R. *J. Org. Chem.* **1973**, *38*, 3862.

(18) Huisgen, R. In *1,3-Dipolar Cycloaddition Chemistry*; Padwa, A., Ed.; Wiley-Interscience: New York, 1984; Chapter 1; p 136.

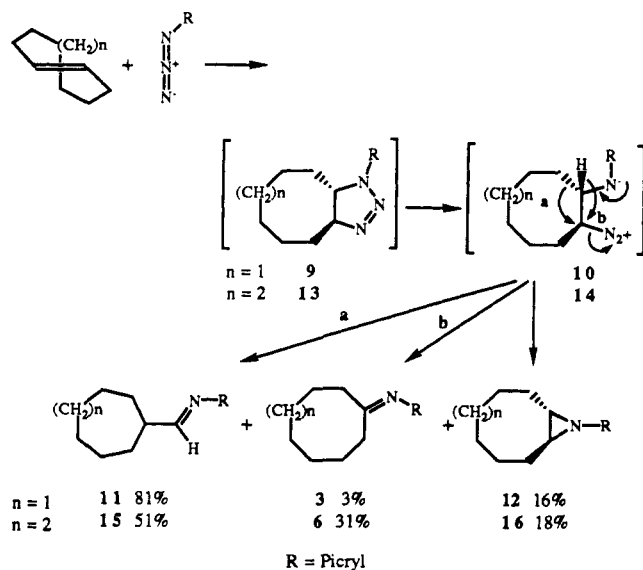
(19) Huisgen, R.; Möbius, L.; Szeimies, G. *Chem. Ber.* **1966**, *99*, 475.

(20) Kalinowski, H.; Kessler, H. *Top. Stereochem.* **1972**, *7*, 295.

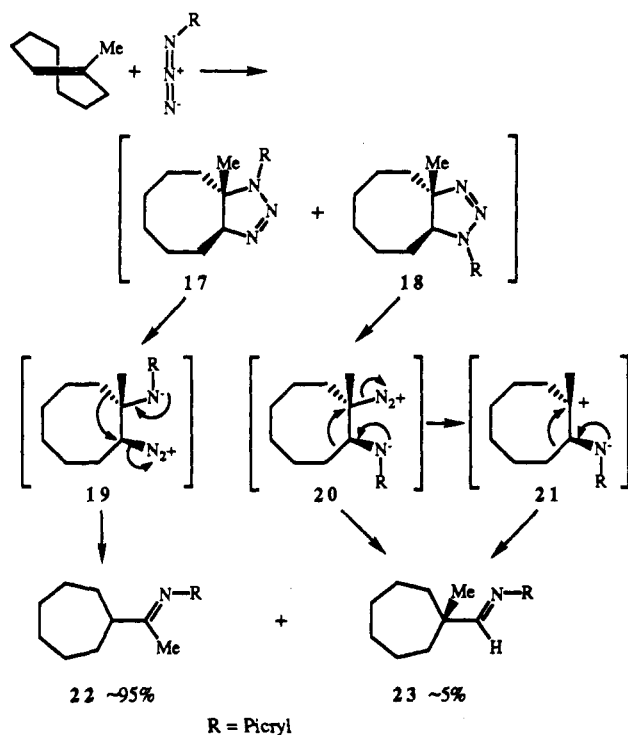
(21) Bailey, A. S.; Wedgwood, J. J. *J. Chem. Soc. C* **1968**, 682.

(22) Hermes, M. E.; Marsh, F. D. *J. Org. Chem.* **1972**, *37*, 2969.

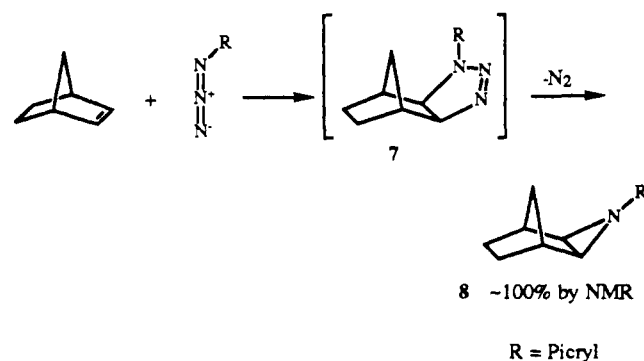
Scheme II



Scheme III



The picryl azide addition to norbornene also gave a single product, the exo aziridine (8) as had been reported previously.²¹⁻²³



Scheme IV

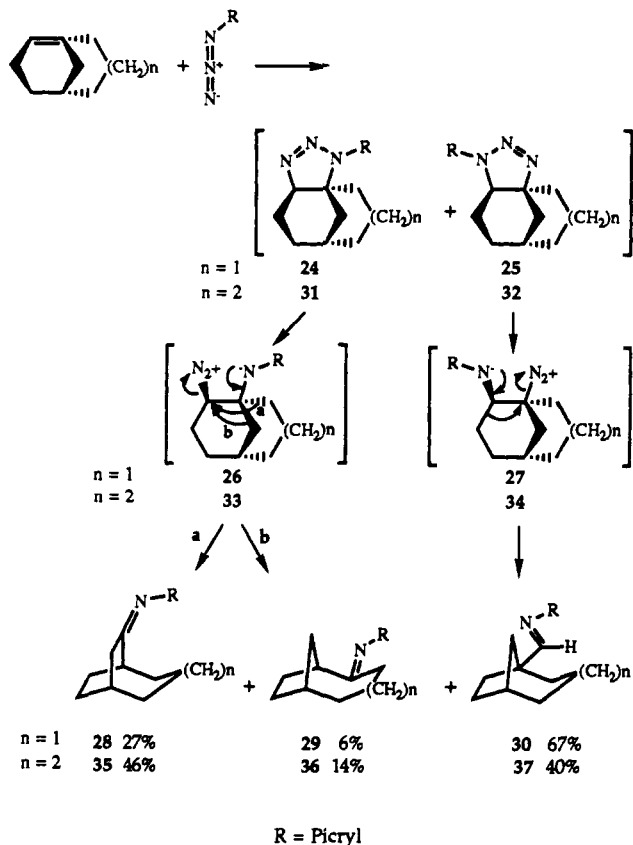


Table I. Product Distribution for the Addition of Azides to Trisubstituted Olefins

olefin	picryl azide ^a		phenyl azide	
	syn:anti		syn:anti	
1-methylcyclopentene (45)			100:0 ^b	
1-methyl- <i>trans</i> -cyclooctene (47)		95:5	100:0 ^b	
bicyclo[4.3.1]dec-1(9)-ene (48)		60:40	66:34 ^c	
bicyclo[3.3.1]non-1-ene (49)		33:67	33:67 ^b	
bicyclo[4.2.1]non-1(8)-ene (50)			45:55 ^b	
bicyclo[4.2.1]non-1-ene (51)			33:67 ^b	

^a This work, in CHCl_3 . ^b Reference 24, in pentane. ^c This work, in pentane.

Reaction of picryl azide with *trans*-cyclooctene and *trans*-cyclononene gave three products, aldimines (11 and 15) which arise from alkyl migration of the zwitterions 10 and 14, ketimines (3 and 6) from hydride migrations, and *trans*-aziridines (12 and 16). No traces of *cis*-fused aziridines could be found (Scheme II).

1-Methyl-*trans*-cyclooctene gave mostly ketimine 22, which is derived from syn cycloadduct 17, and aldimine 23 from anti cycloadduct 18 (Scheme III). Formation of 22, a product of ring alkyl migration from zwitterion 19, is similar to the migration products from *trans*-cyclooctene and *trans*-cyclononene.

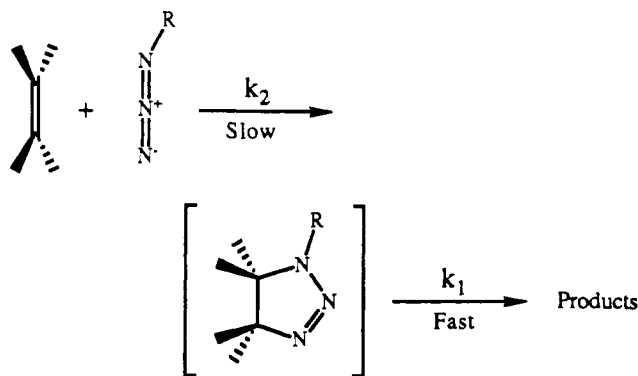
Bicyclo[3.3.1]non-1-ene and bicyclo[4.3.1]dec-1(9)-ene each gave three products: ketimine 28 (35) from the syn cycloadduct 24 (31) and subsequent migration of the alkyl ring, ketimine 29 (36) from 24 (31) and migration of the methylene bridge, and aldimine 30 (37) from the anti cycloadduct 25 (32) and subsequent migration of the alkyl ring (Scheme IV). Ratios of these products are somewhat less reliable because of overlapping peaks in the

¹H-NMR spectrum that prevented accurate integration.

B. Regiochemistry. The product distributions of triazoline cycloadducts with picryl azide and phenyl azide are summarized in Table I. Product ratios of picryl azide addition are derived from analysis of the rearranged products. The product ratios of phenyl azide additions are those of Becker et al.²⁴ The similar ratios for the two azides suggest that both reactions proceed by similar mechanisms.

Bridgehead olefins (**48** and **49**) in the picryl azide addition produce significant amounts of anti cycloadducts (Table I). This result differs from that obtained for reference alkenes, since alkyl-substituted unsymmetrical olefins give almost exclusive syn cycloaddition (Introduction). This anomaly with bridgehead olefins is in contrast with the results from 1-methyl-*trans*-cyclooctene (**47**), which gave only small amounts of the anti cycloadduct.

C. Kinetic Studies. Second-order rate constants for picryl azide addition to olefins in CHCl₃ were measured by UV absorbance. Pseudo-first-order reaction rates were determined using a 10–100-fold excess of olefin. In some cases, second-order reaction rates were determined directly. In these cases, identical concentrations were used. The change in the concentration of picryl azide vs time was measured by the absorbance of picryl azide at 298 nm in all runs except for bicyclo[3.3.1]non-1-ene, which was measured at 273 nm. Absorbance was measured directly in a thermostated cell except for reactions with cyclooctene, in which reaction mixtures were quenched with an excess of solvent and transferred immediately to a UV cell to measure the absorbance. The activation parameters may have considerable uncertainty because rate constants were obtained at three temperatures.



The triazoline adduct of bicyclo[3.3.1]non-1-ene could be detected, permitting direct second-order reaction rates. A different wavelength (273 nm) was used to monitor the reaction in this case to avoid interference of the intermediate triazoline. The 273-nm wavelength was chosen because this corresponds to an isosbestic point for product and intermediate.

The results of the kinetic experiments are summarized in Table II. Literature values for the rate constants of cyclooctene and norbornene are 9.32×10^{-5} and $2.04 \times 10^{-2} \text{ L mol}^{-1} \text{ s}^{-1}$ at 25 °C in CHCl₃ by IR kinetic experiments.²⁵ Our results fit within 10% (8.31×10^{-5} and $1.92 \times 10^{-2} \text{ L mol}^{-1} \text{ s}^{-1}$ at 25 °C in CHCl₃, UV method) of these values.

Discussion

Product Studies. The triazoline cycloadducts are unstable to the reaction conditions. They react with loss of nitrogen to produce imines and aziridines. The ratio of products is quite substrate dependent. We attempt to analyze the origin of the product ratios in terms of zwitterionic intermediates (i.e., A–D, Figure 2) that have a sufficient lifetime to permit bond rotation to be competitive with migration and loss of N₂. The evidence for this mechanism is compelling since the products do not reflect a synchronous *trans*-antiperiplanar migration and N₂ loss from the *initial* zwitterion.

Table II. Second-Order Rate Constants and Kinetic Parameters for Picryl Azide Addition Reactions to Olefins in CHCl₃

Olefin	k_2^a (25°C) (L mol ⁻¹ sec ⁻¹)	k_{rel}^b	E_a^c (kcal/mol)	ΔS^\ddagger^c (eu)
(38) ^d	1.08×10^{-4}	42.4		
(39) ^d	2.55×10^{-6}	1		
(40) ^d	1.36×10^{-4}	53.3		
(41)	$8.31 \pm 0.31 \times 10^{-5}$	65.2	13.3 ^d	-34.3 ^d
(42)	$1.92 \pm 0.08 \times 10^{-2}$	1.50×10^4	9.8 ± 0.5	-35.5 ± 1.7
(43)	$1.29 \pm 0.05 \times 10^{-2}$	1.01×10^4	12.2 ± 0.5	-28.4 ± 1.7
(44)	$6.87 \pm 0.22 \times 10^{-1}$	5.39×10^5	11.2 ± 0.4	-23.7 ± 1.3
(45) ^d	2.99×10^{-5}	11.7		
(46) ^d	4.07×10^{-5}	16.0		
(47)	1.05 ± 0.01	8.24×10^5	8.6 ± 0.2	-31.6 ± 0.5
(48)	$5.82 \pm 0.60 \times 10^{-3}$	4.56×10^3	9.5 ± 1.4	-38.9 ± 4.5
(49)	50.5 ± 1.7	3.96×10^7	6.1 ± 0.5	-32.3 ± 1.7

^a Errors are in 95% confidence limit. ^b Statistically corrected, see ref 1b. ^c Errors are calculated from the slope of the least-squares line of $\ln k$ vs $1/T$ plot; see: Shoemaker, D. P.; Garland, C. W.; Steinfeld, J. I. *Experiments in Physical Chemistry*; McGraw-Hill: New York, 1974; p 55. ^d Reference 25.

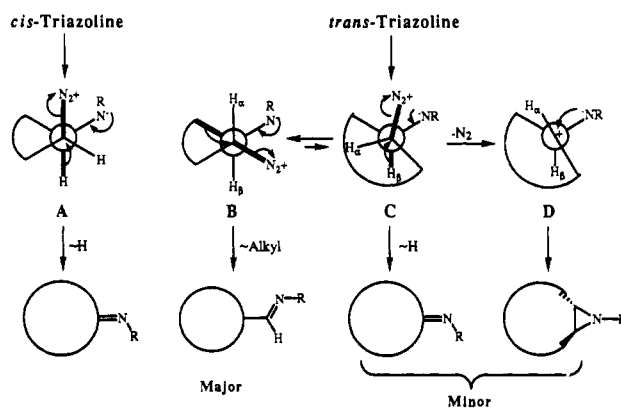


Figure 2. Conformational analysis for the product formation of *cis*- and *trans*-triazolines.

A similar situation appears to exist in the related semipinacol rearrangement.²⁶ A satisfactory accounting of the product ratio is obtained by assuming that the transition state energy for the product-forming step parallels the relative stability of the zwitterions. For example, *cis*-cycloalkene adducts decompose via hydride migration to produce the exocyclic imine (Figure 2). *trans*-Cycloalkene adducts, however, react mainly by alkyl migration. This finding can be explained by zwitterionic intermediates with rate constants for conformational relaxation that are competitive with decomposition (Figure 2). *cis*-Triazolines would produce initially intermediate A in which hydrogen is antiperiplanar to the departing diazonium ion. Rearrangement would result in the hydride shift product. *trans*-Triazolines, on the other hand, are expected to exist in conformers B and C, in which B is the more stable conformer in small- and medium-ring systems as a result of the backside strain in the ring. The stability of B increases as the ring size becomes smaller, and conformer C is not important in small-ring systems. The product ratios of 11:3

(24) Becker, K. B.; Hohermuth, M. K. *Helv. Chim. Acta* **1979**, *62*, 2025.

(25) Bailey, A. S.; White, J. E. *J. Chem. Soc. B* **1966**, 819.

(26) Stevens, T. S.; Watts, W. E. In *Selected Molecular Rearrangements*; Van Nostrand Reinhold Company: London, 1973; Chapter 2.

(27) Winkler, F. K.; Dunitz, J. D. *J. Mol. Biol.* **1971**, *59*, 169.

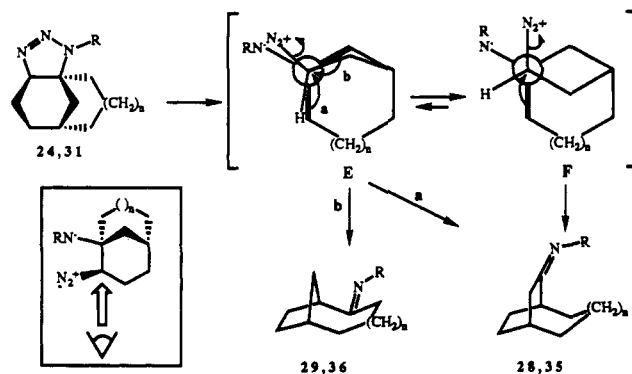


Figure 3. Mechanism of the decomposition of syn cycloadducts 24 and 31.

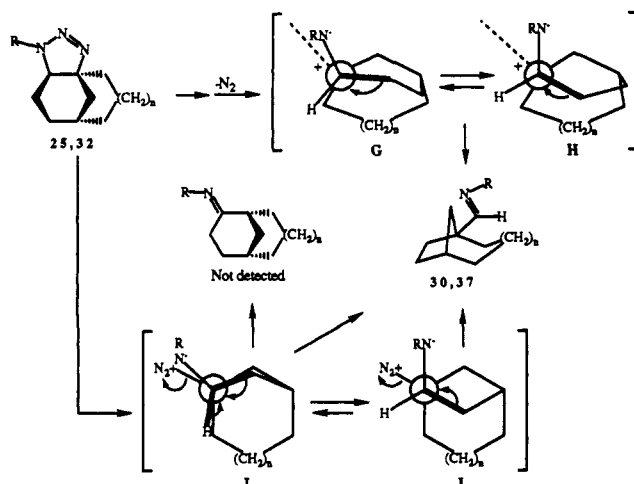


Figure 4. Mechanism of the decomposition of anti cycloadducts 25 and 32.

and 15:6 reflect this situation, that is, alkyl migration exceeds hydride migration slightly in the nine-membered-ring system (15:6 = 51:31), and alkyl migration dominates in the eight-membered-ring system (11:3 = 81:3).

In 1-methyl-*trans*-cyclooctene, the absence of a methyl migration product suggests that reaction from conformer B (Figure 2, $H_\beta = \text{CH}_3$) is favored to produce ketimine 22 (Scheme III),

possibly because of the additional steric hindrance of the methyl group to the ring to make conformer C less favored (Figure 2, $H_\beta = \text{CH}_3$). Regiochemistry of the initial azide addition is normal (syn:anti = 17:18 = 95:5) because syn adduct 17 is expected to be the favored product from a consideration of the interaction between the LUMO of the azide and HOMO of the olefin.¹¹

Product formation from the decomposition of syn cycloadducts 24 and 31 can be explained by the transition states resulting from rearrangement of conformers E and F shown in Figure 3. The initially formed conformer E can produce two products via either ring alkyl migration (mode a) or methylene bridge migration (mode b). The chances of forming either product in a kinetically controlled reaction from conformer E are similar because of similar attack angles. Bond rotation to give the more stable conformer F, in which only the ring alkyl group would be expected to migrate, should enhance the amount of 28 (35). Product ratios (28:29 = 27:6 = 4.5:1 and 35:36 = 46:14 = 3.3:1), suggest time for equilibration because compounds 28 and 35 dominate. Rearrangement may occur slightly faster than bond rotation (or the transition state energies may not parallel the conformational stabilities) because the difference of MM-2 steric energy between models of conformers E and F ranges about 2 kcal/mol (see second row in Figure 5), which would allow an equilibrium composition of F:E = 97:3 at room temperature.

Product formation from the decomposition of anti cycloadducts 25 and 32 seems to proceed mainly via free carbocation intermediates G and H (Figure 4) because a single isomeric product 30 (37) was found. Rearrangement via zwitterion conformers I and J would be expected to produce two products as in the case of the syn cycloadduct, and the ratios of products from the hydride migration of conformer I should not be less than that found in the syn cycloadducts because the steric energy difference between conformers I and J is expected to be less than that between E and F in the syn cycloadducts (see third row in Figure 5). Free carbocation intermediates G and H, on the other hand, have only one possible migrating mode resulting in formation of 30 and 37. The conformations of G and H were estimated with MM-2 minimized structures containing an sp^2 center at the bridgehead position. Obviously, the driving force for free carbocations in this case is formation of the more stable tertiary carbocation. This result parallels examples involving related 1,2-rearrangements. For example, fully developed carbocations are involved in the pinacol rearrangement to tertiary centers. In contrast, diazonium ions are involved at secondary centers.²⁶

Regiochemistry of Additions. The regiochemistry of picryl azide cycloadditions to bridgehead alkenes deviates from the predictions

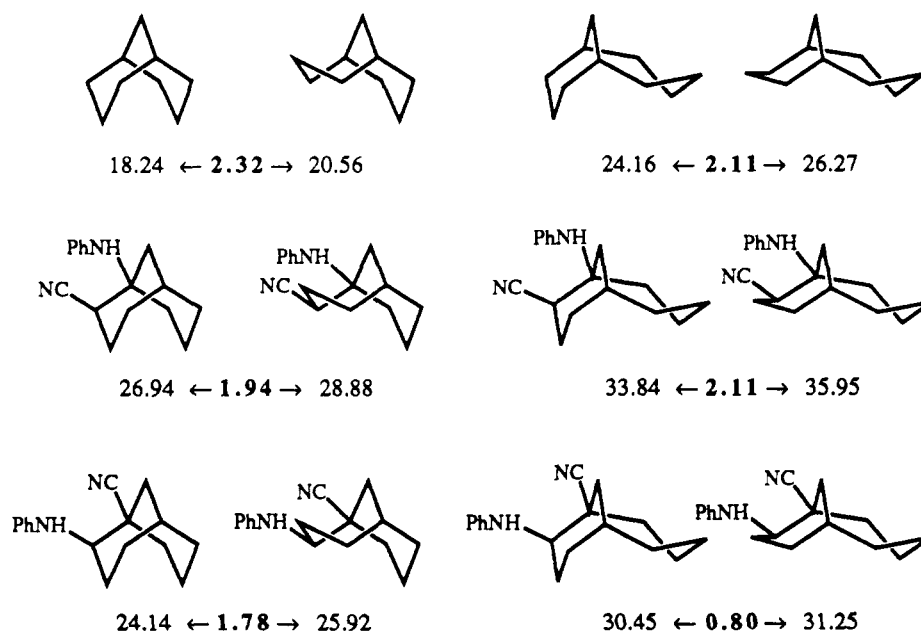


Figure 5. MM-2 steric energies of conformational isomer models (kcal/mol).

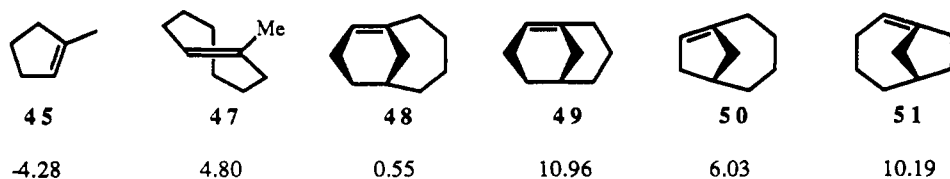


Figure 6. Olefin strains (kcal/mol) of trisubstituted alkenes by MM-2 calculation. Olefin strain = steric energy of olefin - steric energy of corresponding alkane.

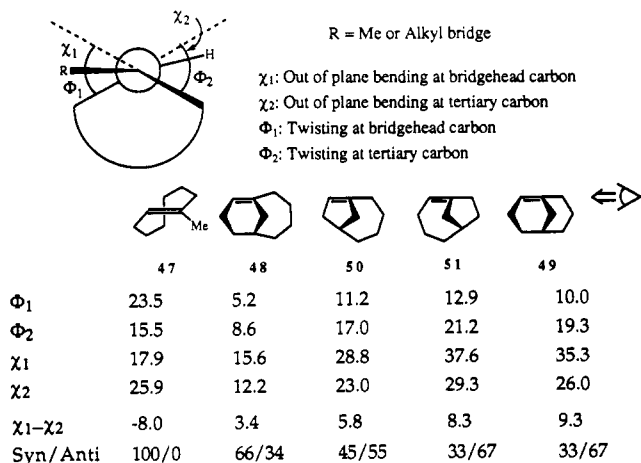


Figure 7. Deformation angles (deg) of strained trisubstituted olefins calculated by MM-2. Pyramidalization angles (χ) were calculated by the dihedral angles, so they are slightly larger than the real pyramidalization angle.²⁷ Syn:anti ratios are for the phenyl azide additions.

of FMO theory. Steric hindrance cannot be a major factor influencing this change because the olefins in Table I comprise an isosteric series. Most strained bridgehead olefins (i.e., 49) give a higher than expected proportion of the anti cycloadduct. Strain itself, however, is not the only factor since bicyclo[4.3.1]dec-1-(9)-ene (48) gives a higher ratio of the anti cycloadduct than 1-methyl-*trans*-cyclooctene (47) even though 47 is more strained (Figure 6).

An important difference between *trans*-cycloalkenes and bridgehead olefins is that the double bond in *trans*-cycloalkenes is deformed mainly by twisting, whereas the double bonds in the bridgehead olefins have additional deformations as a result of pyramidalization (out of plane bending) by the alkyl bridge in addition to twisting. As a result of this additional deformation, the π -orbital in bridgehead olefins would become more unsymmetrical. Deformation angles calculated by MM-2 were obtained and compared with product ratios of azide additions (Figure 7).

The out of plane bending angle (χ_1 and χ_2) of the strained olefins shows a difference between 1-methyl-*trans*-cyclooctene (47) and bridgehead olefins. Though magnitudes vary, all bridgehead olefins have greater out of plane bending angles at the bridgehead position than at the sp^2 position adjacent to the bridgehead ($\chi_1 > \chi_2$). 1-Methyl-*trans*-cyclooctene (47), however, has a smaller out of plane bending angle at the tertiary position ($\chi_1 < \chi_2$). When the product ratios (syn:anti) for phenyl azide addition are compared with the difference of the out of plane bending angles ($\chi_1 - \chi_2$), a qualitative relationship is found. As the difference in out of plane bending angles ($\chi_1 - \chi_2$) becomes greater, the proportion of the syn cycloadduct becomes higher. This result implies that the out of plane bending distortion influences the orbital picture, especially the orbital coefficients of the HOMO of the double

bond, despite the fact that the orbital energy is not very sensitive to the distortions.²⁸

Kinetic Studies. The reactivity of strained olefins is significantly higher than that of simple unstrained cycloalkenes (Table II). The reactivity of *trans*-cyclooctene (44) is even higher than that of norbornene (42). This is interesting since norbornene has been treated as an exceptional case because of its high reactivity in Diels-Alder reactions and 1,3-dipolar cycloadditions.²⁹ The entropy of activation (ΔS^\ddagger) increases from *cis*-cyclooctene to *trans*-cycloalkenes. This could be due to one or both of two possible factors: the more reactive *trans*-cycloalkenes may have an earlier transition state, and the reactant is more organized in the *trans*-cycloalkenes than in the *cis*-cycloalkenes.

In comparison with disubstituted cycloalkenes, the trisubstituted olefins such as 1-methylcyclopentene (45) and 1-methylcycloheptene (46) show lower reactivities (0.28 and 0.30). This decrease in reactivity upon methyl substitution is perhaps due to the steric hindrance of an additional methyl group since addition of an alkyl group should increase the HOMO energy of an olefin (ca. 0.6 eV),³⁰ which in turn should result in an increase in cycloaddition rate. The reversal of this trend for 1-methyl-*trans*-cyclooctene (47) vs *trans*-cyclooctene (44) ($k_{1\text{-methyl-}trans\text{-cyclooctene}}/k_{trans\text{-cyclooctene}} = 1.5$) could be due to the looser transition state for *trans*-cycloalkenes ($\Delta S^\ddagger_{cis\text{-cyclooctene}} = -34.3$ eu and $\Delta S^\ddagger_{trans\text{-cyclooctene}} = -23.7$ eu), resulting in a less important role for steric interactions.

In comparison with our previous epoxidation studies,^{1b} the spread in reactivity is greater. For example, relative rate constants of cyclohexene (39):*trans*-cyclooctene (44):bicyclo[3.3.1]non-1-ene (49) are $1:5.39 \times 10^5:3.96 \times 10^7$ in picryl azide additions and $1:4.54 \times 10^2:8.90 \times 10^3$ in MCPBA epoxidations. Evidently, more strain is relieved in the transition state of azide additions.

In order to obtain a measure of the strain energy relieved in the transition state, MM-2 calculations of the steric energy of olefins and their corresponding triazoline model (Figure 8) were performed (Table III).³¹ The energies obtained were based on the most stable conformational isomers. The differences in steric energy between olefins and the corresponding triazoline model (ΔSE) are used to determine the amount of strain energy relieved in the transition state in a manner similar to the approach used in our epoxidation study.¹⁶ The basic assumption is that the energy constrained in an olefin is partially relieved (or acquired if the olefin is more stable than the cycloadduct) in the transition state. The fraction of steric energy relief ($\lambda \Delta SE$, $\lambda < 1$) will affect the chemical reactivity, resulting in an increased reaction rate in highly strained olefins such as *trans*-cycloalkenes and bridgehead olefins. Although the geometry of a product does not reflect the transition state structure exactly, we believe that this approach, utilizing differences in steric energy between olefin and reference compound (ΔSE), is a reasonable way to obtain strain energy relief in the transition state.

In addition to the strain relief, the torsional interactions between forming bonds and adjacent bonds in the transition state are believed to be important. Theoretical calculations of 1,3-dipolar

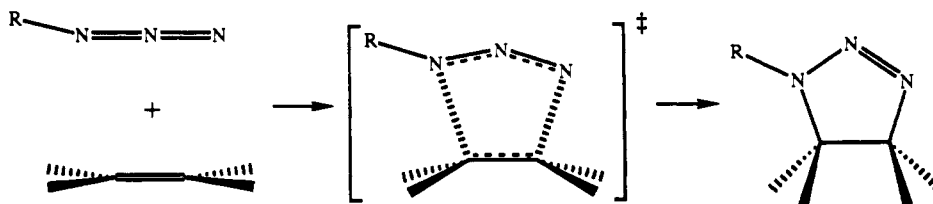
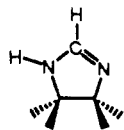


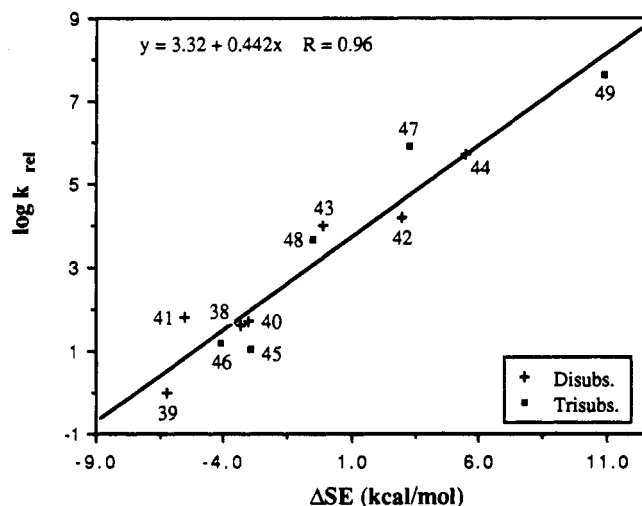
Figure 8. Mechanism of the azide addition reaction.

Table III. MM-2 Minimized Energies of Olefins and Corresponding Triazolines

Triazoline model used ; 

olefin	MM-2 energy ^a			
	k_{rel}	olefin	triazoline ^b	ΔSE^c
cyclopentene (38)	42.4	8.14	11.44	-3.30
cyclohexene (39)	1	4.13	10.39	-6.26
cycloheptene (40)	53.3	9.87	12.92	-3.05
cyclooctene (41)	65.2	13.38	18.90	-5.52
norbornene (42)	1.50×10^4	25.43	22.45	2.98
(<i>E</i>)-cyclononene (43)	1.01×10^4	21.54	21.65	-0.11
(<i>E</i>)-cyclooctene (44)	5.39×10^5	23.17	17.70	5.47
1-methylcyclopentene (45)	11.7	7.26	10.16	-2.90
1-methylcycloheptene (46)	16.0	10.41	14.52	-4.11
1-methyl-(<i>E</i>)-cyclooctene (47)	8.24×10^5	25.06	21.75	3.31
bicyclo[4.3.1]dec-1(9)-ene (48)	4.56×10^3	24.70	25.16 ^d	-0.46
bicyclo[3.3.1]non-1-ene (49)	3.96×10^7	29.19	18.29	10.90

^a Calculated by MacroModel 3.0 program, kcal/mol. ^b Models are used because current program could not calculate triazoline itself; see Figure 8. ^c ΔSE = Steric energy of olefin - steric energy of triazoline. ^d Twisted-boat conformer of six-membered ring; lowest energy is 24.78 kcal/mol with chair conformation of six-membered ring.

**Figure 9.** Correlation between the reactivity and the relief of strain energy in picryl azide addition to an olefin.

cycloadditions reveal that the magnitude of torsional interactions in the transition state are of the same magnitude as in the product, even though the forming bonds are weak and long.³² This effect is also included in the steric energy estimates of the product, making ΔSE a more reliable predictor of transition state energy.

In order to find relationships between the rates of azide addition reactions and relief of strain energy, $\log k_{rel}$ vs ΔSE is plotted in Figure 9. A fair correlation between $\log k_{rel}$ and ΔSE implies that the reactivity increase in *trans*-cycloalkenes and bridgehead alkenes is influenced by the strain relief in the transition state.

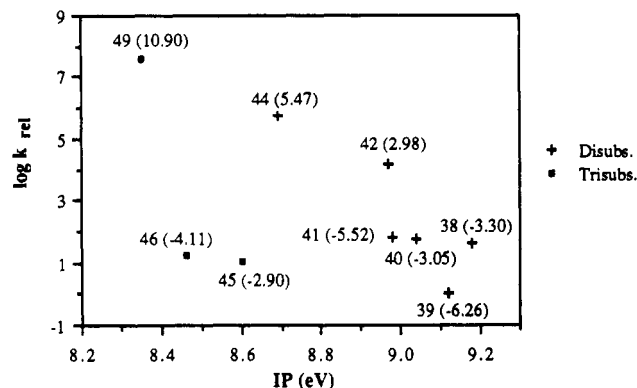
(28) Honegger, E.; Schmelzer, A.; Heilbronner, E. *J. Electron Spectrosc. Relat. Phenom.* **1982**, 28, 79.

(29) Huisgen, R. *Pure Appl. Chem.* **1981**, 53, 171.

(30) Batich, C.; Heilbronner, E.; Quinn, C. B.; Wiseman, J. R. *Helv. Chim. Acta* **1976**, 59, 512.

(31) MM-2 calculations were performed by the MacroModel 3.0 program. Still, W. C. *Macromodel*. Version 3.0. Columbia University, 1990.

(32) (a) Houk, K. N. *Stereochemistry and Reactivity of Systems Containing π Electrons*; Watson, W., Ed.; Verlag Chemie International: New York, 1983; p 1. (b) Rondan, N. G.; Paddon-Row, M. N.; Caramella, P.; Mareda, J.; Mueller, P. H.; Houk, K. N. *J. Am. Chem. Soc.* **1982**, 104, 4974.

**Figure 10.** Plot of reactivity of picryl azide addition reaction vs ionization potential of alkene. Numbers in parentheses are steric energy differences between alkene and triazoline (ΔSE). See ref 1b for ionization potentials. Ionization potential for 1-methylcycloheptene (46) is an extrapolated value.

Norbornene (42) was correlated, indicating that the strain relief is a major factor in its reactivity. Compared with the epoxidation study in which trisubstituted olefins showed a 50-fold increase in reactivity over disubstituted olefins, the azide addition study reveals that both di- and trisubstituted olefins fall on the same correlation line. This could be due to a fortuitous cancellation of the reactivity increase caused by the HOMO energy increase and the reactivity decrease resulting from steric hindrance of additional alkyl groups. From the slope of the correlation between $\log k_{rel}$ and ΔSE (slope = 0.442), which represents the amount of strain relieved in the transition state, a 2.8-fold increase in reaction rate ($=10^{0.442}$) was observed per 1 kcal/mol change in the ΔSE . This reactivity increase amounts to about a 0.60 kcal/mol decrease in the ΔG^\ddagger ($\Delta\Delta G^\ddagger = RT \ln(10^{0.442}) = 0.60$ kcal/mol). Thus, about 60% of the strain energy difference between the olefin and the triazoline (ΔSE) is thought to be relieved in the transition state of picryl azide addition.

In order to find the effect of the difference in olefin HOMO energy on the reactivity with picryl azide, $\log k_{rel}$ vs ionization potential (IP = -HOMO energy) was plotted (Figure 10). Although the rates of some strained olefins appear to correlate with ionization potential, the high reactivity of those olefins should not necessarily be attributed largely to the HOMO energy increase but rather to strain energy relief because the rate increase vs ionization potential is restricted to only highly strained olefins. Less strained olefins do not show any significant increase in reaction rate as the HOMO energy increases. It is, of course, reasonable that some fraction of reactivity is attributed to HOMO energy because azide additions to alkyl-substituted olefins have dominant frontier orbital interactions between the LUMO of the azide and the HOMO of the olefin. However, the HOMO energy could not be a major factor influencing the very large reactivity increase (for example, bicyclo[3.3.1]non-1-ene is 3.96×10^7 times faster than cyclohexene). The reason is that the reactivity changes slowly in the HOMO energy range of alkyl-substituted olefins in azide addition reactions,¹⁰ and the difference of ionization potentials of model olefins in this plot is small (0.83-eV difference). Though it is difficult to establish the contribution of HOMO energy in this plot, the effect is expected to be small as evidenced by the wide spread of points in the $\log k_{rel}$ vs ionization potential plot.

MCPBA Epoxidation vs Picryl Azide Addition. The reactivities of strained alkenes to both MCPBA epoxidation and picryl azide addition are influenced mainly by the strain relief in the transition state as evidenced by the correlation between the reactivity vs ΔSE plot. It was found that up to 40% of the total steric energy difference in the MCPBA epoxidation^{1b} and up to 60% in the picryl azide addition is relieved in the transition state. Although these percentages do not directly reflect the extent of progress along the reaction coordinate, a qualitative prediction is that the transition state in the MCPBA epoxidation is earlier than that in the picryl azide addition.

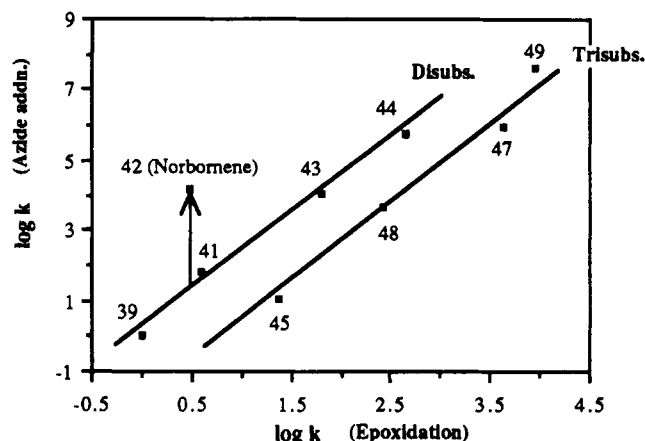


Figure 11. Correlation of the reactivities for the MCPBA epoxidation and the picryl azide addition.

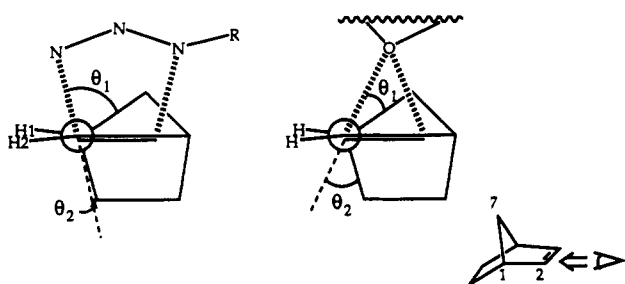


Figure 12. Directions of bond formation for attack of azide and peracid on norbornene.

A direct comparison of the reactivities between azide addition and MCPBA epoxidation is shown in Figure 11. It is not surprising that the di- and trisubstituted olefins correlate well since the reactivity differences in both reactions are caused mainly by the structural changes resulting from the sp^2 to an sp^3 -like transition state. The only large deviation is found for norbornene.

The difference in the reactivity of norbornene between peracid epoxidation and 1,3-dipolar cycloaddition has been used to support Bartlett's concerted epoxidation mechanism and argue against Kwart's 1,3-dipolar mechanism for peracid epoxidations.³³ The good correlation of norbornene in each $\log k_{\text{rel}}$ vs ΔSE plot of the azide addition (Figure 9) and the epoxidation reaction^{1b} suggests that the real cause is simply different patterns of relieving strain in the transition state since the ΔSEs are calculated using structures of both product and olefin.

Why does norbornene differ in reactivity between the MCPBA epoxidation and the picryl azide addition? Theoretical calculations by Houk have shown the importance of torsional interactions between newly forming bonds and adjacent bonds in the transition state. It was found that the torsional interactions in the transition state are of the same order of magnitude as in the product, and the reactivity and selectivity of norbornene depends on these torsional interactions.^{32,34} Major differences between the transition state of epoxidation and that of azide addition are the attack angles (θ_1) of peracid and azide, that is, three-membered rings are made in the peracid epoxidation and five-membered rings are made in azide addition (Figure 12). Therefore, the amount of torsional interaction between forming bonds and existing carbon-carbon bonds in the methylene bridge in norbornene should be different because of the difference in these angles.

The deviation of norbornene from the correlation line of disubstituted olefins as shown in Figure 12 (about 3.9 kcal/mol) may be roughly compared with the estimated values of the eclipsing torsional interaction energy on the rigid polycyclic systems, estimated to be 2–5 kcal/mol.³⁴ Hyperconjugation³⁵ is also able

to affect the reactivity of norbornene, since in the transition state of the azide addition there is a good antiperiplanar relationship between forming bonds and the C_1-C_6 (C_4-C_5) bonds (θ_2 in Figure 12), but this is not the case in the epoxidation. It is difficult to separate torsional effects and hyperconjugation in these systems because the smaller contribution from hyperconjugation (larger θ_2) gives rise to increased torsional interactions (smaller θ_1). Regardless, the torsional interaction is expected to be a major factor since the reactivities of norbornene correlate well with $\log k_{\text{rel}}$ vs ΔSE plots for both epoxidation and azide addition even though the MM-2 energy does not contain a hyperconjugative contribution but does contain a torsional effect.

Conclusion

The addition of picryl azide to a series of mono- and bicyclic olefins including *trans*-cycloalkenes and bridgehead alkenes was studied. Products were identified, and their mechanism of formation was explained by an analysis of the conformation of zwitterionic reaction intermediates. Bridgehead alkenes show a reversal from the normal trend of regiochemistry compared with model alkenes. It is proposed that the reversal is caused by the out of plane bending of the bridgehead double bond.

The kinetics of the cycloaddition reveals significant increases in the reaction rate of picryl azide addition to strained olefins. A good correlation was found in the plot of $\log k_{\text{rel}}$ vs ΔSE , where ΔSE values were calculated from differences of MM-2 steric energy between olefins and the corresponding triazolines. This finding indicates that the strain relief in the transition state is a major factor affecting the reactivity of alkyl-substituted mono- and bicyclic olefins. The HOMO energy change did not affect the reactivity significantly in the picryl azide addition to alkyl-substituted olefins as evidenced by the absence of correlation in $\log k_{\text{rel}}$ vs ionization potential. Up to 60% of the steric energy difference (ΔSE) is found to be relieved in the transition state from the slope of the $\log k_{\text{rel}}$ vs ΔSE plots.

By comparison of the reaction rates for the MCPBA epoxidation and the picryl azide addition, reactivity patterns were found to be similar among the olefins studied, except for norbornene. A possible explanation for the norbornene abnormality calls attention to the torsional interactions that develop between forming bonds and existing carbon-carbon bonds in the methylene bridge.

An important outcome of this research is the quantification of the effect of strain on chemical reactivity and selectivity. The strain involved in an olefin changes both reactivity and regiochemistry. These results can be explained by the local deformation of carbon-carbon double bonds resulting in influences on the orbital shape and energy.

Experimental Section

Proton NMR spectra were obtained with Bruker WM 250 (250 MHz) and General Electric QE-300 (300 MHz) spectrometers. Chemical shifts are reported in δ -units with tetramethylsilane as an internal reference for ^1H -NMR. Coupling constants are reported in hertz (Hz) and refer to apparent multiplicities. Carbon NMR spectra were obtained with General Electric QE-300 (75.43 MHz) and GN-500 (125.7 MHz) spectrometers. Low-resolution mass spectra were obtained with a Finnigan Model 4000 GC/MS instrument using a 70-eV electron impact source or a 100-eV chemical ionization source. High-resolution mass spectra were obtained with a VG 7070e high-resolution mass spectrometer by the UC—Irvine staff. Infrared spectra were recorded on an Analect RFX-40 FT-IR spectrophotometer and calibrated with polystyrene. UV-vis spectra were obtained with a Perkin Elmer Lambda-4 spectrometer, and data were collected and analyzed with the Softways UVSL 4 program. Molecular mechanics calculations were performed by the MacroModel version 3.0 program on a microvax computer.

Syntheses of olefins were carried out using the same method as in ref 1b.

2-Nitrophenyl Azide. A mixture of *o*-nitroaniline (28 g, 0.20 mol), water (80 mL), and concentrated HCl (45 mL, 0.54 mol) was placed in a 500-mL flask. The flask was cooled to 0 °C, and then NaNO_2 (14.5 g, 0.21 mol) in water (50 mL) was added dropwise. After 1 h of stirring at 0 °C, the yellow solution was suction filtered from the trace of in-

(33) Bingham, K. D.; Meakins, G. D.; Whitham, G. H. *Chem. Commun.* **1966**, 445.

(34) Caramella, P.; Rondan, N. G.; Paddon-Row, M. N.; Houk, K. N. *J. Am. Chem. Soc.* **1981**, *103*, 2438.

(35) (a) Cieplak, A. S.; Tait, B. D.; Johnson, C. R. *J. Am. Chem. Soc.* **1989**, *111*, 8447. (b) Cieplak, A. S. *J. Am. Chem. Soc.* **1981**, *103*, 4540.

soluble impurities and poured into a 2-L beaker surrounded by an ice bath. With stirring, NaN_3 (13 g, 0.20 mol) in 50 mL of water was added. Immediately the product began to precipitate as a light cream. After the nitrogen evolution had ceased, the product was collected on a Buchner funnel. Washing with cold water and drying gave 30 g of crude 2-nitrophenyl azide²⁵ (91%), which could be used in the next step without further purification: $^1\text{H-NMR}$ (CDCl_3) δ 7.93 (dd, $J = 8.2, 1.5$ Hz, 1 H), 7.64 (ddd, $J = 8.2, 7.5, 1.5$ Hz, 1 H), 7.35 (dd, $J = 8.2, 1.2$ Hz, 1 H), 7.27 (ddd, $J = 8.2, 7.5, 1.2$ Hz, 1 H); $^{13}\text{C-NMR}$ (CDCl_3) δ 140.72, 134.62, 133.96, 125.92, 124.83, 120.68; IR (cm^{-1} , CCl_4) 2135 (s), 2121 (s), 2098 (m), 1616 (w), 1604 (m), 1583 (w), 1535 (s), 1508 (w), 1489 (m), 1353 (m), 1317 (m), 1297 (m), 1167 (w).

2,4,6-Trinitrophenyl Azide (Picryl Azide).²⁵ To a well-stirred mixture of HNO_3 (25 mL, fuming, 90%) and H_2SO_4 (25 mL, concentrated), which had been cooled to 0 °C, was added 2-nitrophenyl azide (5.0 g, 31 mmol). After being stirred at 0 °C for 1 h, the reaction mixture was poured onto ice, and the solid was collected and washed with water. Quick recrystallization from methanol gave 4.4 g (56%) of the azide: mp 89–90 °C dec; $^1\text{H-NMR}$ (CDCl_3) δ 8.93 (s, 2 H); $^{13}\text{C-NMR}$ (CDCl_3) δ 144.0, 142.5, 133.9, 123.9 ($J_{\text{CH}} = 177$ Hz); IR (cm^{-1} , CCl_4) 3097 (w), 2158 (m), 2131 (m), 1610 (m), 1552 (s), 1543 (s), 1458 (w), 1342 (s), 1288 (w), 1182 (w), 1120 (w); UV (λ_{max} , nm, CHCl_3) 297 ($\epsilon = 11400$); CI-MS (isobutane, relative percent) m/e 255 ($M + 1$, 10), 227 ($MH^+ - N_2$, 100), 213 (54), 199 (99); EI-MS (relative percent) m/e 254 (2), 226 ($M - N_2$, 14), 196 (42), 120 (18), 87 (49), 76 (41), 75 (39), 74 (100), 73 (15), 64 (16), 63 (14), 62 (70), 61 (90), 53 (17), 51 (15), 50 (20).

Picryl Azide Addition to *cis*-Cyclooctene. *cis*-Cyclooctene (65.2 mg, 0.592 mmol) was mixed with picryl azide (100 mg, 0.394 mmol) in chloroform (2 mL) and kept dark for 5 days. Crude $^1\text{H-NMR}$ showed formation of a single product. Purification by flash chromatography (230–400-mesh SiO_2 , 1:1 hexane:chloroform) afforded cyclooctylidene-2,4,6-trinitroaniline (**3**)²⁰ (122 mg, 92%).

Cyclooctylidene-2,4,6-trinitroaniline (3**):** $^1\text{H-NMR}$ (CDCl_3) δ 9.00 (s, aryl CH, 2 H), 2.52 (m, $\text{HCC}=\text{N}$, 4 H), 1.84 (br, 4 H), 1.58 (br, 6 H); $^{13}\text{C-NMR}$ (CDCl_3) δ 186.97 ($\text{C}=\text{N}$), 143.78 (quaternary aryl carbon), 139.98 (quaternary aryl carbon), 139.10 (quaternary aryl carbon), 124.74 (aryl CH), 37.37, 27.14, 25.50, 24.61; IR (cm^{-1} , CCl_4) 3097 (w), 2935 (m), 2860 (w), 1672 (m, $\text{C}=\text{N}$ stretching), 1612 (s), 1593 (s), 1543 (s), 1468 (w), 1446 (w), 1410 (w), 1340 (s), 1296 (m), 1217 (w), 1176 (w), 1155 (w), 1080 (m), 935 (w), 910 (m); EI-MS (relative percent) m/e 337 ($M + 1$, 2), 336 (M , 8), 238 (3), 221 (4), 116 (3), 107 (3), 97 (7), 96 (3), 95 (18), 83 (6), 81 (22), 79 (8), 75 (6), 74 (7), 69 (14), 67 (18), 57 (7), 56 (9), 55 (100), 54 (6), 53 (8); HR-MS (EI) calcd for $\text{C}_{14}\text{H}_{16}\text{N}_4\text{O}_6$: 336.1069. Found: 336.1056.

Picryl Azide Addition to *cis*-Cyclononene. *cis*-Cyclononene (24.4 mg, 0.197 mmol) was mixed with picryl azide (50.0 mg, 0.197 mmol) in chloroform (1 mL) and kept dark for 7 days. Crude $^1\text{H-NMR}$ showed formation of a single product. Purification by flash column chromatography (230–400-mesh SiO_2 , 1:1 hexane:chloroform) afforded cyclononylidene-2,4,6-trinitroaniline (**6**) (57.8 mg, 84%).

Cyclononylidene-2,4,6-trinitroaniline (6**):** yellow crystals; mp 63–64 °C; $^1\text{H-NMR}$ (CDCl_3) δ 9.00 (s, aryl OH, 2 H), 2.53 (m, $\text{HCC}=\text{N}$, 4 H), 1.84 (br, 4 H), 1.63 (br, 4 H), 1.53 (br, 2 H); $^{13}\text{C-NMR}$ (CDCl_3) δ 187.14 ($\text{C}=\text{N}$), 143.63 (quaternary aryl carbon), 140.00 (quaternary aryl carbon), 139.14 (quaternary aryl carbon), 124.76 (aryl CH), 38.47, 26.23, 24.91, 24.36; IR (cm^{-1} , CCl_4) 3097 (w), 2929 (m), 2873 (w), 2854 (w), 1670 (m, $\text{C}=\text{N}$ stretching), 1612 (s), 1593 (s), 1543 (s), 1479 (w), 1446 (w), 1410 (w), 1340 (s), 1296 (m), 1230 (w), 1176 (w), 1157 (w), 1144 (w), 1082 (m), 939 (w), 920 (m); CI-MS (isobutane, relative percent) m/e 351 ($M + 1$, 32), 141 (100); EI-MS (relative percent) m/e 350 (M , 4), 239 (12), 238 (24), 221 (17), 196 (9), 139 (18), 124 (11), 123 (100), 122 (10), 121 (14), 97 (16), 95 (51), 93 (25), 91 (13), 89 (12), 85 (10), 84 (10), 83 (29), 82 (14), 81 (81), 80 (17), 79 (36), 77 (20), 75 (25), 74 (29), 71 (19), 70 (19); HR-MS (EI) calcd for $\text{C}_{15}\text{H}_{18}\text{N}_4\text{O}_6$: 350.1226, found 350.1225.

Picryl Azide Addition to Norbornene. Norbornene (100 mg, 1.04 mmol) was added dropwise into a solution of picryl azide (240 mg, 0.945 mmol) in chloroform (5 mL), and the reaction mixture was kept dark for 1 day. Crude $^1\text{H-NMR}$ showed formation of a single product. Purification by flash column chromatography (230–400 mesh SiO_2 , 1:1 hexane:chloroform) afforded aziridine **8** (260 mg, 86%).

3-2',4',6'-Trinitrophenyl-3-azatricyclo[3.2.1.0^{2,4}]octane (8**):**²⁰ $^1\text{H-NMR}$ (CDCl_3) δ 8.90 (s, aryl CH, 2 H), 2.82 (s, 2 H), 2.61 (s, 2 H), 1.60 (br d, $J = 9$ Hz, 2 H), 1.48 (br d, $J = 10.5$ Hz), 1.24 (dd, $J = 8, 2$ Hz, 2 H), 1.08 (d, $J = 10.5$ Hz); $^{13}\text{C-NMR}$ (CDCl_3) δ 145.10 (quaternary aryl carbon), 141.40 (quaternary aryl carbon), 136.60 (quaternary aryl carbon), 125.24 (aryl CH), 46.40, 36.18, 29.46, 24.98.

Picryl Azide Addition to *trans*-Cyclooctene. *trans*-Cyclooctene (95.0 mg, 0.862 mmol) was added dropwise into a solution of picryl azide (219

mg, 0.862 mmol) in chloroform (10 mL) and kept dark for 1 h. Purification by flash column chromatography (230–400-mesh SiO_2 , 1:1 hexane:chloroform) afforded two different fractions. The first fraction ($R_f = 0.4$ by TLC with 1:1 hexane:chloroform) was identified as aldimine **11** (181 mg, 62%), and the second fraction was a mixture of aziridine **12** and imine **3** ($R_f = 0.27$ by TLC with 1:1 hexane:chloroform). Pure aziridine **12** (23 mg, 8%) was obtained by recrystallization with 1:1 hexane:chloroform. A trace of imine **3** was found in the remaining solution.

(Cycloheptylmethylidene)-2,4,6-trinitroaniline (11**):** yellow crystals; mp 60–61 °C; $^1\text{H-NMR}$ (CDCl_3) δ 8.94 (s, aryl CH, 2 H), 7.97 (d, $J = 4.6$ Hz, $\text{HC}=\text{N}$, 1 H), 2.65 (ttd, $J = 9.0, 4.5, 4.5$ Hz, $\text{HCC}=\text{N}$, 1 H), 2.1–1.95 (m, 2 H), 1.95–1.7 (m, 2 H), 1.75–1.5 (m, 8 H); $^{13}\text{C-NMR}$ (CDCl_3) δ 178.26 ($\text{C}=\text{N}$), 145.79 (quaternary aryl carbon), 141.06 (quaternary aryl carbon), 140.97 (quaternary aryl carbon), 123.79 (aryl CH), 46.54 ($\text{HCC}=\text{N}$), 29.52, 28.41, 26.08; IR (cm^{-1} , CCl_4) 3097 (m), 2931 (s), 2858 (m), 1682 (m, $\text{C}=\text{N}$ stretching), 1612 (s), 1597 (m), 1545 (s), 1460 (w), 1446 (w), 1412 (w), 1340 (s), 1300 (w), 1221 (w), 1182 (w), 1080 (w), 937 (w), 918 (w); CI-MS (isobutane, relative percent) m/e 337 ($M + 1$, 43), 113 (100); EI-MS (relative percent) m/e 336 (M , 1), 225 (13), 224 (10), 97 (12), 95 (24), 81 (20), 80 (15), 79 (17), 69 (12), 67 (32), 55 (100), 53 (12); HR-MS (EI) calcd for $\text{C}_{14}\text{H}_{16}\text{N}_4\text{O}_6$: 336.1069, found 336.1070. Imine **11** in acetone changed slowly to a dark red compound, which is assumed to be an enamine form by NMR spectra.

2',4',6'-Trinitrophenyl-*trans*-2-azabicyclo[6.1.0]nonane (12**):** light yellow crystals; mp 216–217 °C; $^1\text{H-NMR}$ (CDCl_3) δ 8.91 (s, aryl CH, 2 H), 2.58 (m, protons at aziridine ring, 2 H), 2.25 (m, 2 H), 2.08 (m, 2 H), 1.94 (m, 2 H), 1.52 (m, 2 H), 1.08–0.94 (m, 4 H); $^{13}\text{C-NMR}$ (CDCl_3) δ 146.00 (quaternary aryl carbon), 142.41 (quaternary aryl carbon), 137.57 (quaternary aryl carbon), 124.96 (aryl CH), 51.39, 30.69, 28.98, 27.73; IR (cm^{-1} , CCl_4) 3097 (w), 2939 (m), 2862 (w), 1610 (s), 1591 (m), 1541 (s), 1475 (w), 1458 (w), 1448 (w), 1414 (w), 1340 (s), 1298 (w), 1267 (w), 1234 (w), 1211 (w), 1169 (w), 1086 (w); CI-MS (isobutane, relative percent) m/e 337 ($M + 1$, 98), 109 (100); EI-MS (relative percent) m/e 336 (M , 1), 225 (13), 95 (19), 81 (27), 80 (14), 79 (20), 77 (15), 75 (13), 69 (23), 67 (43), 57 (14), 56 (10), 55 (100), 54 (16), 53 (18); HR-MS (EI) calcd for $\text{C}_{14}\text{H}_{16}\text{N}_4\text{O}_6$: 336.1069, found 336.1054.

Picryl Azide Addition to *trans*-Cyclononene. *trans*-Cyclononene (30.0 mg, 0.241 mmol) was added dropwise into a solution of picryl azide (61.4 mg, 0.241 mmol) in chloroform (2 mL) and kept dark for 1 day. Purification by flash column chromatography (230–400-mesh SiO_2 , 1:1 hexane:chloroform) afforded two fractions. The first fraction ($R_f = 0.4$ by TLC with 1:1 hexane:chloroform) was identified as aldimine **15** (29.8 mg, 35%), and the second fraction was a mixture of aziridine **16** and imine **6** ($R_f = 0.25$ by TLC with 1:1 hexane:chloroform). Pure aziridine **16** (10.7 mg, 13%) was obtained by recrystallization with 1:1 hexane:chloroform. Imine **6** was found in the remaining solution.

(Cyclooctylmethylidene)-2,4,6-trinitroaniline (15**):** $^1\text{H-NMR}$ (CDCl_3) δ 8.94 (s, aryl CH, 2 H), 7.96 (d, $J = 4.6$ Hz, $\text{HC}=\text{N}$, 1 H), 2.69 (ttd, $J = 8.4, 4.2, 4.2$ Hz, $\text{HCC}=\text{N}$, 1 H), 2.03–1.92 (m, 2 H), 1.85–1.5 (m, 12 H); $^{13}\text{C-NMR}$ (CDCl_3) δ 178.63 ($\text{C}=\text{N}$), 145.80 (quaternary aryl carbon), 141.03 (quaternary aryl carbon), 140.95 (quaternary aryl carbon), 123.78 (aryl CH), 45.19 ($\text{HCC}=\text{N}$), 27.32, 26.81, 25.95, 24.93; IR (cm^{-1} , CCl_4) 3097 (m), 2925 (s), 2856 (m), 1682 (m, $\text{C}=\text{N}$ stretching), 1614 (s), 1597 (m), 1542 (s), 1475 (w), 1448 (w), 1410 (w), 1340 (s), 1300 (m), 1219 (w), 1182 (w), 1080 (m), 1012 (w), 935 (w), 918 (m); EI-MS (relative percent) m/e 350 (M , 3), 225 (24), 224 (7), 127 (12), 109 (16), 95 (14), 93 (19), 83 (10), 82 (9), 81 (35), 80 (9), 79 (20), 77 (11), 69 (44), 68 (11), 67 (64), 57 (15), 55 (100), 54 (12), 53 (17); HR-MS (EI) calcd for $\text{C}_{15}\text{H}_{18}\text{N}_4\text{O}_6$: 350.1226, found 350.1221. Imine **15** in acetone changed slowly to a dark red compound, which is assumed to be an enamine form by NMR spectra.

2',4',6'-Trinitrophenyl-*trans*-2-azabicyclo[7.1.0]decane (16**):** light yellow crystals; mp 176–179 °C; $^1\text{H-NMR}$ (CDCl_3) δ 8.88 (s, aryl CH, 2 H), 2.62 (m, protons at aziridine ring, 2 H), 2.20 (m, 2 H), 1.97 (m, 2 H), 1.70 (m, 2 H), 1.46 (m, 2 H), 1.36–1.16 (m, 4 H), 0.85 (m, 2 H); $^{13}\text{C-NMR}$ (CDCl_3) δ 145.73 (quaternary aryl carbon), 142.56 (quaternary aryl carbon), 137.59 (quaternary aryl carbon), 124.81 (aryl CH), 51.62, 30.44, 29.62, 24.02, 22.72; IR (cm^{-1} , CCl_4) 3097 (w), 2941 (m), 2871 (w), 1610 (s), 1591 (s), 1540 (s), 1470 (m), 1452 (w), 1414 (w), 1340 (s), 1296 (m), 1255 (w), 1243 (w), 1176 (w), 1134 (w), 1086 (w); CI-MS (isobutane, relative percent) m/e 351 ($M + 1$, 100), 141 (51), 123 (37); EI-MS (relative percent) m/e 237 (5), 225 (10), 123 (9), 95 (13), 93 (12), 81 (28), 79 (15), 77 (11), 75 (10), 69 (28), 68 (10), 67 (47), 57 (15), 56 (11), 55 (100), 54 (16), 53 (15); HR-MS (EI) calcd for $\text{C}_{15}\text{H}_{18}\text{N}_4\text{O}_6$: 350.1226, found 350.1249.

Picryl Azide Addition to 1-Methyl-*trans*-cyclooctene. 1-Methyl-*trans*-cyclooctene (50.5 mg, 0.410 mmol) was added dropwise into a

solution of picryl azide (94.7 mg, 0.372 mmol) in chloroform (2 mL) and kept dark for 1 h. Purification by flash column chromatography (230–400-mesh SiO₂, 1:1 hexane:chloroform) afforded the imine **22** contaminated with a trace of **23** (*R_f* = 0.4 by TLC with 1:1 hexane:chloroform). Pure imine **22** (96.3 mg, 74%) was obtained by recrystallization with 2:1 hexane:chloroform.

1'-Cycloheptylethylidene-2,4,6-trinitroaniline (22): yellow crystals: mp 116–117 °C; ¹H-NMR (CDCl₃) δ 8.99 (s, aryl CH, 2 H), 2.56 (tt, *J* = 9.6, 3.8 Hz, HCC=N, 1 H), 2.10 (s, CH₃, 3 H), 2.0 (m, 2 H), 1.8 (m, 2 H), 1.7–1.45 (m, 8 H); ¹³C-NMR (CDCl₃) δ 185.42 (C=N), 145.02 (quaternary aryl carbon), 139.92 (quaternary aryl carbon), 139.60 (quaternary aryl carbon), 124.49 (aryl CH), 50.26 (HCC=N), 31.27, 28.05, 26.59, 23.66 (CH₃); IR (cm⁻¹, CCl₄) 3097 (w), 2931 (m), 2858 (w), 1687 (m, C=N stretching), 1612 (s), 1593 (m), 1545 (s), 1462 (w), 1446 (w), 1410 (w), 1340 (s), 1298 (w), 1176 (w), 1161 (w), 1082 (w), 920 (w); CI-MS (isobutane, relative percent) *m/e* 351 (*M* + 1, 77), 141 (100); EI-MS (relative percent) *m/e* 281 (13), 251 (30), 240 (11), 239 (99), 238 (26), 223 (10), 212 (26), 205 (11), 197 (22), 196 (32), 193 (18), 139 (71), 138 (14), 131 (14), 123 (15), 121 (16), 120 (11), 97 (38), 96 (18), 95 (62), 93 (22), 91 (14), 89 (20), 83 (45), 82 (19), 81 (100), 80 (46), 79 (40), 77 (28), 76 (13), 75 (25), 74 (44), 71 (11); HR-MS (CI) calcd for C₁₅H₁₉N₄O₆ 351.1304, found 351.1297.

[(1-Methylcycloheptyl)methylidene]-2,4,6-trinitroaniline (23). Compound **23** was not purified, so the identification was done on the trace of the NMR spectra of the mixture. Although not complete, only five different sp³ carbons, including one quaternary carbon in the ¹³C-NMR spectrum, clearly indicate the correct assignment because of the symmetry of compound **23**. A sharp singlet peak at 7.9 ppm in the ¹H-NMR spectrum shows the presence of an imine aldehyde proton: ¹H-NMR (CDCl₃) δ 8.9 (s, aryl CH, 2 H), 7.9 (s, HC=N, 1 H), 1.18 (s, CH₃, 3 H); ¹³C-NMR (CDCl₃) δ 181.36 (C=N), 123.67 (aryl CH), 45.0 (quaternary, CC=N), 36.44, 30.47, 24.90, 22.79.

Picryl Azide Addition to Bicyclo[3.3.1]non-1-ene. Bicyclo[3.3.1]non-1-ene (25.3 mg, 0.207 mmol) was added dropwise into a solution of picryl azide (47.8 mg, 0.188 mmol) in chloroform (2 mL), and the reaction mixture was stirred for 30 min. Purification by flash column chromatography (230–400-mesh SiO₂, 1:1 hexane:chloroform) afforded two different fractions. The first fraction (*R_f* = 0.33 by TLC with 1:1 hexane:chloroform) was identified as aldimine **30** (32.9 mg, 50%), and the second fraction (*R_f* = 0.24 by TLC with 1:1 hexane:chloroform) was a mixture of imine **28** and imine **29** (16.1 mg, 24%).

(1-Bicyclo[3.2.1]octylmethylidene)-2,4,6-trinitroaniline (30): yellow crystals; mp 104–106 °C; ¹H-NMR (CDCl₃) δ 8.94 (s, aryl CH, 2 H), 7.94 (s, HC=N, 1 H), 2.42 (br, bridgehead proton, 1 H), 1.91 (m, 2 H), 1.9–1.4 (m, 10 H); ¹³C-NMR (CDCl₃) δ 179.98 (C=N), 146.23 (quaternary aryl carbon), 141.02 (quaternary aryl carbon), 140.92 (quaternary aryl carbon), 123.80 (aryl CH), 50.89 (CC=N), 42.24, 35.90, 32.88, 31.80, 31.72, 29.12, 18.83; IR (cm⁻¹, CCl₄) 3097 (w), 2943 (m), 2871 (w), 2858 (w), 1680 (m, C=N stretching), 1614 (s), 1597 (m), 1545 (s), 1456 (w), 1410 (w), 1340 (s), 1300 (w), 1219 (w), 1078 (w), 935 (w), 918 (w); CI-MS (isobutane, relative percent) *m/e* 349 (*M* + 1, 24), 139 (100); EI-MS (relative percent) *m/e* 319 (2), 305 (2), 225 (9), 224 (6), 125 (54), 109 (47), 107 (20), 95 (17), 93 (18), 92 (10), 91 (23), 83 (15), 81 (48), 80 (21), 79 (67), 77 (30), 75 (10), 74 (11), 69 (10), 68 (10), 67 (100), 66 (11), 65 (19), 57 (10), 55 (55), 53 (28); HR-MS (EI) calcd for C₁₅H₁₈N₄O₆ 348.1069, found 348.1043.

6'-Bicyclo[3.2.2]nonylidene-2,4,6-trinitroaniline (28): ¹H-NMR (CDCl₃) δ 9.01 (s, aryl CH, 2 H), 2.79 (br, bridgehead HCC=N, 1 H), 2.47 (m, H₂CC=N, 2 H), 2.27 (br, bridgehead proton, 1 H), 2.1–1.6 (m, 10 H); ¹³C-NMR (CDCl₃) δ 187.98 (C=N), 144.54 (quaternary aryl carbon), 140.03 (quaternary aryl carbon), 139.60 (quaternary aryl carbon), 124.63 (aryl CH), 43.02, 39.88, 33.57, 31.12, 28.44, 23.63, 22.78, 21.32.

Picryl Azide Addition to Bicyclo[4.3.1]dec-1(9)-ene. Bicyclo[4.3.1]dec-1(9)-ene (46.3 mg, 0.340 mmol) was added dropwise into a solution of picryl azide (78.5 mg, 0.309 mmol) in chloroform (2 mL), and the reaction mixture was stirred for 1 day. Purification by flash column chromatography (230–400-mesh SiO₂, 1:1 hexane:chloroform) afforded two different fractions. The first fraction (*R_f* = 0.4 by TLC with 1:1 hexane:chloroform) was identified as aldimine **37** (34.3 mg, 31%), and the second fraction (*R_f* = 0.25 by TLC with 1:1 hexane:chloroform) was a mixture of imine **35** and imine **36** (46.5 mg, 42%). Pure imine **35** (29.8 mg, 27%) was obtained by recrystallization with 1:1 hexane:chloroform. Imine **36** was identified by the recrystallization residue.

(1-Bicyclo[4.2.1]nonylmethylidene)-2,4,6-trinitroaniline (37): ¹H-NMR (CDCl₃) δ 8.94 (s, aryl CH, 2 H), 7.95 (s, HC=N, 1 H), 2.6 (br, bridgehead proton, 1 H), 2.2–2.0 (m, 2 H), 2.0–1.4 (m, 12 H); ¹³C-NMR

(CDCl₃) δ 180.54 (C=N), 146.09 (quaternary aryl carbon), 140.97 (quaternary aryl carbon), 140.84 (quaternary aryl carbon), 123.80 (aryl CH), 53.44 (CC=N), 38.07, 37.39, 36.33, 35.07, 34.85, 33.51, 25.10, 24.70; IR (cm⁻¹, CCl₄) 3097 (w), 2924 (m), 2862 (w), 1680 (m, C=N stretching), 1614 (s), 1597 (m), 1545 (s), 1462 (w), 1452 (w), 1410 (w), 1340 (s), 1300 (w), 1219 (w), 1078 (w), 937 (w), 918 (w); CI-MS (isobutane, relative percent) *m/e* 363 (*M* + 1, 49), 153 (100); EI-MS (relative percent) *m/e* 319 (17), 225 (15), 212 (7), 139 (43), 133 (10), 123 (19), 122 (13), 121 (34), 109 (16), 107 (16), 105 (12), 97 (13), 95 (33), 94 (13), 93 (56), 92 (11), 91 (32), 83 (16), 82 (9), 81 (99), 80 (49), 79 (70), 78 (10), 77 (29), 75 (10), 69 (22), 68 (11), 67 (100), 66 (11), 65 (20), 55 (81), 53 (32); HR-MS (EI) calcd for C₁₆H₁₈N₄O₆ 362.1223, found 362.1244.

7'-Bicyclo[4.2.2]decylidene-2,4,6-trinitroaniline (35): orange crystals; mp 154–156 °C; ¹H-NMR (CDCl₃) δ 9.01 (m, aryl CH, 2 H), 2.89 (br, bridgehead HCC=N, 1 H), 2.65 (dd, *J* = 18.7, 7.1 Hz, H₂CC=N, 1 H), 2.43 (br, bridgehead proton, 1 H), 2.30 (d, *J* = 18.8 Hz, H₂CC=N, 1 H), 2.04 (m, 2 H), 1.9–1.5 (m, 9 H), 1.42 (m, 1 H); ¹³C-NMR (CDCl₃) δ 189.02 (C=N), 144.14 (quaternary aryl carbon), 139.96 (quaternary aryl carbon), 139.59 (quaternary aryl carbon), 138.80 (quaternary aryl carbon), 124.94 (aryl CH), 124.74 (aryl CH), 42.09, 37.49, 37.19, 35.74, 28.53, 24.68, 24.08, 24.00, 23.01; IR (cm⁻¹, CCl₄) 3097 (w), 2925 (m), 2870 (w), 1674 (m), 1612 (s), 1593 (m), 1543 (s), 1450 (w), 1408 (w), 1338 (s), 1294 (w), 1213 (w), 1138 (w), 1080 (w), 939 (w), 920 (w); CI-MS (isobutane, relative percent) *m/e* 363 (*M* + 1, 60), 153 (100); EI-MS (relative percent) *m/e* 363 (5), 362 (M, 22), 238 (8), 221 (8), 123 (11), 121 (15), 109 (17), 108 (12), 107 (19), 105 (11), 96 (16), 95 (30), 93 (47), 91 (25), 83 (10), 82 (26), 81 (100), 80 (29), 79 (75), 77 (26), 75 (12), 74 (14); HR-MS (EI) calcd for C₁₆H₁₈N₄O₆ 362.1223, found 362.1211.

2'-Bicyclo[5.2.1]decylidene-2,4,6-trinitroaniline (36): ¹H-NMR (CDCl₃) δ 8.94 (m, aryl CH, 2 H), 2.94 (br t, bridgehead HCC=N, 1 H), 2.67 (m, H₂CC=N, 1 H), 2.47–2.37 (br m, 2 H), 2.2–2.0 (m, 2 H), 2.0–1.5 (m, 8 H), 1.43 (m, 1 H), 1.3 (m, 1 H); ¹³C-NMR (CDCl₃) δ 186.40 (C=N), 124.26 (aryl CH), 124.10 (aryl CH), 48.24, 36.34, 34.54, 31.90, 30.36, 27.27, 26.16, 25.03, 23.73; HR-MS (CI) calcd for C₁₆H₁₉N₄O₆ (*M* + 1) 363.1301, found 363.1313.

Method of Kinetics. Rate constants were measured spectrophotometrically by monitoring the disappearance of picryl azide absorption. Pseudo-first-order reaction rates were measured for most kinetic experiments. Direct second-order reaction rates were measured for the reaction involving bicyclo[3.3.1]non-1-ene. The rate equations used are as follows:

$$\text{rate} = k_2[\text{olefin}][\text{azide}]$$

$$\ln [\text{azide}]_t = -k_1 t + \ln [\text{azide}]_0 \text{ when } [\text{olefin}] \gg [\text{azide}], k_1 = k_2[\text{olefin}]$$

$$1/[\text{azide}]_t = k_2 t + 1/[\text{azide}]_0 \text{ when } [\text{olefin}] = [\text{azide}]$$

A Perkin-Elmer Lambda-4 spectrometer equipped with a thermostated cell was used. The concentration changes were obtained by the absorbance of picryl azide at 298 nm or at 268 nm. The absorbances were corrected by the blank solutions containing the olefins. Kinetic experiments involving cyclooctene were performed by keeping the solution in a thermostated bath, taking aliquots and diluting to proper concentrations, and reading the absorbances at suitable intervals. In other cases, the kinetic experiments were performed by reading the absorbance of the solution remaining in the UV cell at suitable time intervals. In a typical kinetic run, measured amounts of olefin and picryl azide in CHCl₃ which had been maintained at suitable temperature for 15–30 min were mixed and immediately transferred to the UV cell, which also had been maintained at the same temperature. The absorbance was monitored immediately. For faster reactions, the picryl azide solution (or the olefin solution) was kept in the UV cell and mixed with the other solution inside the UV cell. Infinite time readings (*A_∞*) were made after 8–10 half-lives. The energy and entropy of activation (*E_a* and Δ*S*[‡]) were calculated by the Arrhenius plot (ln *k* vs 1/*T*) at 25 °C as shown below.

$$\ln k = -E_a/RT + \ln A$$

$$\text{slope} = -E_a/R \quad E_a = -R(\text{slope})$$

$$\text{intercept} = \ln A \quad \Delta S^\ddagger = R[\ln A - \ln (k_B T/h) - 1]$$

Acknowledgment. We are grateful to the Chemistry Division of the National Science Foundation for financial support.